Determining the material model at elevated temperatures with different strain rates and simulating the warm forming process for Mg alloy AZ31B sheet

- **Truong Tich Thien**
- **Nguyen Thanh Long**
- **Vu Nguyen Thanh Binh**
- **Nguyen Thai Hien**

Ho Chi Minh city University of Technology, VNU-HCM

(Manuscript Received on August 01st, 2015, Manuscript Revised August 27th, 2015)

ABSTRACT:

Magnesium alloy is one of lightweight alloys has been studied more extensively today. Because weight reduction while maintaining functional requirements is one of the major goals in industries in order to save materials, energy and costs, etc. Its density is about 2/3 of aluminum and 1/4 of steel.The material used in this study is commercial AZ31B magnesium alloy sheet which includes 3% Al and 1% Zn. However, due to HCP (Hexagonal Close-Packed) crystal structure, magnesium alloy has limited ductility and poor formability at room temperature. But its ductility and formability will be improved clearly at elevated temperature. From the data of tensile testing, the constitutive equations of AZ31B was approximated using the Ramgberg-Osgood model with temperature-dependent parameters to fit in the experiment results in tensile test. Yield locus are also drawn in plane stress $\sigma 1$-$\sigma 2$ with different yield criteria such as Hill48, Drucker Prager, Logan Hosford, Y. W. Yoon 2013 and particular Barlat 2000 criteria with temperature-dependent parameters. Applying these constitutive equations were determined at various temperatures and different strain rates, the finite element simulation stamping process for AZ31B alloy sheet by software PAM- STAMP 2G 2012, to verify the model materials and the constitutive equations.

Key words: *Magnesium alloy sheet, AZ31B, constitutive equation, strain hardening, Ramgberg- Osgood, Barlat 2000, finite element method.*

1. INTRODUCTION

Magnesium alloys are increasingly becoming the ideal materials for modern industrial products with the characteristics of light weight and recycling. Because of lower density, better collision safety property and electromagnetic interference shielding capability, magnesium alloys are available for producing some structural parts such as the covering of mobile telephones, note book computers and potable mini disks. In the past, the demand for

this alloy as a structural material was not high because of its less availability commercially as well as limited manufacturing methods. Recently, die casting of magnesium alloys has been the prevailing method for manufacturing pasts in the automotive industry [1]. However, this process is not ideal in producing thin-walled Mg structures because of excessive amount of waste materials and casting defects. So sheet metal forming processes (such as thermal deep-drawing process, isothermal gas forming) have been developed to manufacture thin-walled parts with good mechanical property and surface quality to avoid the defects above [1].

Deep - drawing process is an important and popular process in assessment of formability of sheet metal. Magnesium possesses poor formability at room temperature. One of the reasons for the poor formability is that the number of independently deformation modes for the basal slip, which is the dominant slip system of hexagonal close-packed (HCP) crystal structure at room temperature is only two while at least five independent slip systems are necessary for homogeneous deformation of polycrystalline material (von Mises 1928). It is necessary to enhance the forming temperatures in order to improve formability of magnesium alloys effectively [1]. Unlike the room temperature behavior, ductility and formability are greatly improved with elevated temperature above 200 - 300^0C [2]. Because of the activation of the pyramidal slip systems, in addition, forming at elevated temperature lowers punch force and blank springback, see the Fig. 1. It can be demonstrated that elevated temperatures contribute firstly to improved ductility and hence forming capability, and secondly that this strategy can help reduce the yield point of the material and hence the forming forces and pressures required **[**3**]**.

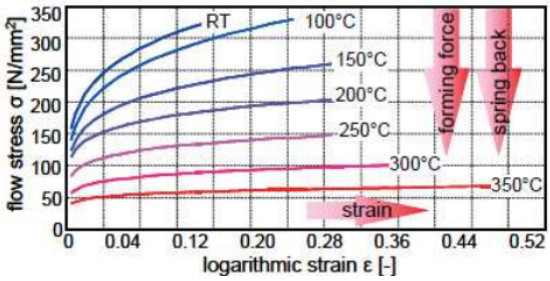

Figure 1. Effect of elevated temperatures on the flow curve of magnesium [3]

At room temperature, magnesium alloy sheets have a significant anisotropy that deviates from conventional predictions using von Mises or Hill yield surfaces. In addition, annealed magnesium alloy sheets have lower compressive yield strength than the tensile strength and concave-up compressive hardening behavior. This behavior is caused by the pyramidal twining which is activated at low temperature. At high temperature, on the other hand, the degree of asymmetric and anisotropy is greatly reduced. The material model for magnesium alloy sheets should be able to describe these anisotropy, asymmetry and temperature dependent behavior. The different strain- stress curves in rolling and transverse direction is shown in Fig. 2

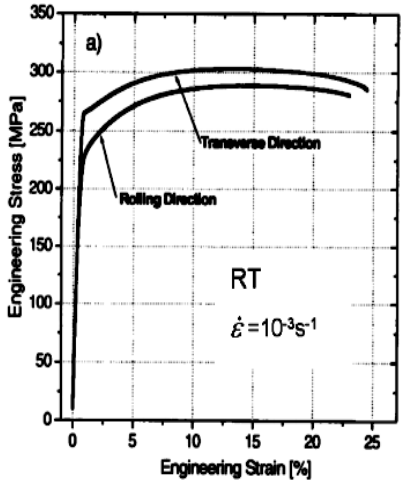

Figure 2. Strain stress curve in rolling and transverse direction at RT [4].

Finite element method (FEM) is a very effective method to simulation the forming processes with accurate prediction of the deformation behaviors. FEM can be used not only in the analysis but also in the design to estimate the optimum conditions of the forming processes. This can be done before carrying out the actual experiments for an economical and successful application of superplastic forming (SPF) to industrial components. In this paper, the simulation of the hot forming process for Mg alloy AZ31B sheet is on PAM- STAMP2G software.

2. CONSTITUTIVE EQUATIONS AT ELEVATED TEMPERATURES AND DIFFERENT STRAIN RATE

2.1. Hardening curve

The flow stress equation is identified with stress and strain data in order to describe the deformation behavior of metal and analyzed by Ramberg-Osgood model (1943) (E_0 is Young's Modulus, $\sigma_{0.2}$ is the offset 0.2 % yield stress, n is the exponent- parameter), as shown in Fig. 3(a) [5].

$$\varepsilon = \frac{\sigma}{E_0} + 0.002\left(\frac{\sigma}{\sigma_{0.2}}\right)^n \quad (1)$$

Assumes that an exponential relationship exists between stress (σ) and plastic strain(ε_p).

$$\varepsilon^p = 0.002\left(\frac{\sigma}{\sigma_{0.2}}\right)^n \Rightarrow \sigma = \left(\frac{\sigma_{0.2}}{(0.002)^{1/n}}\right)\left(\varepsilon^p\right)^{1/n} \quad (2)$$

Taking the logarithm to base 10 of Eq.(2) is obtained as Eq.(3), from the reference data [6], represented in logarithm scale, Fig. 3(b) show the linear relationship between log(ε_p) and log(σ).

$$\log\sigma = \log\left(\frac{\sigma_{0.2}}{(0.002)^{1/n}}\right) + \frac{1}{n}\log\varepsilon^p \quad (3)$$

From the transformed equation Eq.(3) is obtained which can be analyzed by the method of linear regression, to approximate the value of the Ramberg-Osgood parameters (E_0 , $\sigma_{0.2}$, n). The result of an approximate value as shown in Table. 1, the maximum error can be accepted (4.3399 % in 100°C curve). The Ramberg-Osgood parameters at any temperature (from 25°C to 250°C) are approximated by high-order polynomial interpolation from 5 sets of parameters which are approximated from the experimental data. The stress-strain curves of AZ31B alloy at various temperatures are plotted and formed the characteristic strip of the stress-strain curves, as shown in Fig. 4(a). From the Ramberg-Osgood parameters also are used to form the stress-plastic strain curves with different strain rate to describe the hardening behavior of AZ31B alloy sheet, as shown in Fig. 4(b).

Table. 1 Maximum error between the approximate and experimental curve

t°(°C)	E_0 (GPa)	$\sigma_{0.2}$ (MPa)	n	Max error (%)
25	43.1	179	7.5579	**2.8895**
100	38.1	126	10.2528	**4.3399**
150	32.2	94.6	13.2994	**4.2139**
200	29.8	56.2	19.9510	**2.9933**
250	29.0	33.6	12.3167	**2.4277**

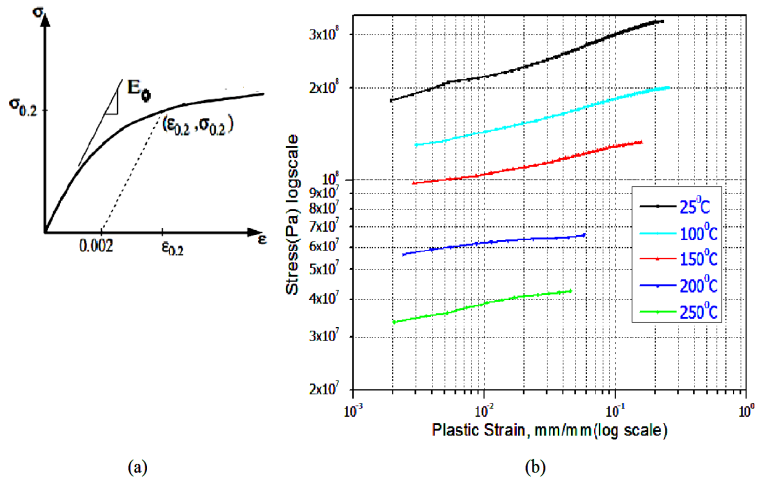

Figure. 3. (a) Generic representation of the stress-strain curve by Ramberg-Osgood means clustering of the equation. (b) The linear relationship between $\log(\varepsilon^p)$ and $\log(\sigma)$

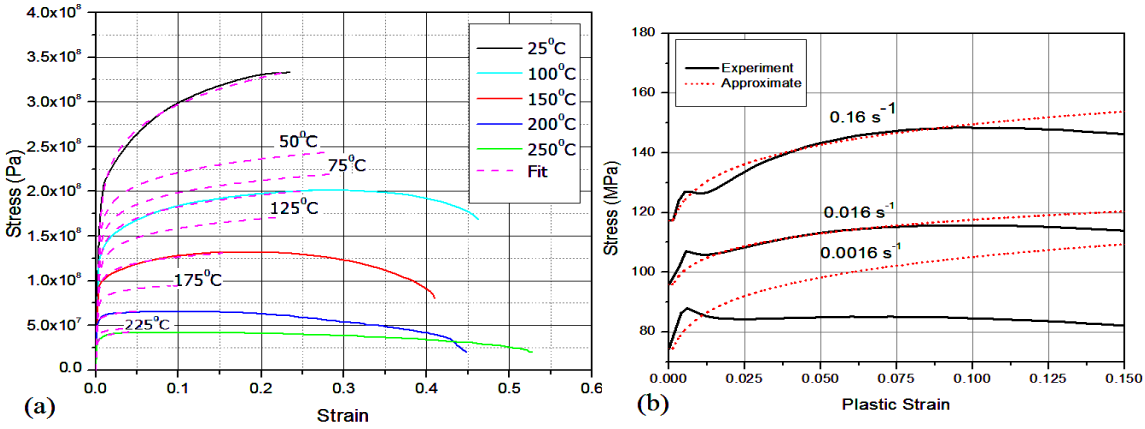

Figure. 4. (a) Stress-strain curves of AZ31B alloy at any temperature, (b) Stress-plastic strain curves at 150°C with difference strain rate.

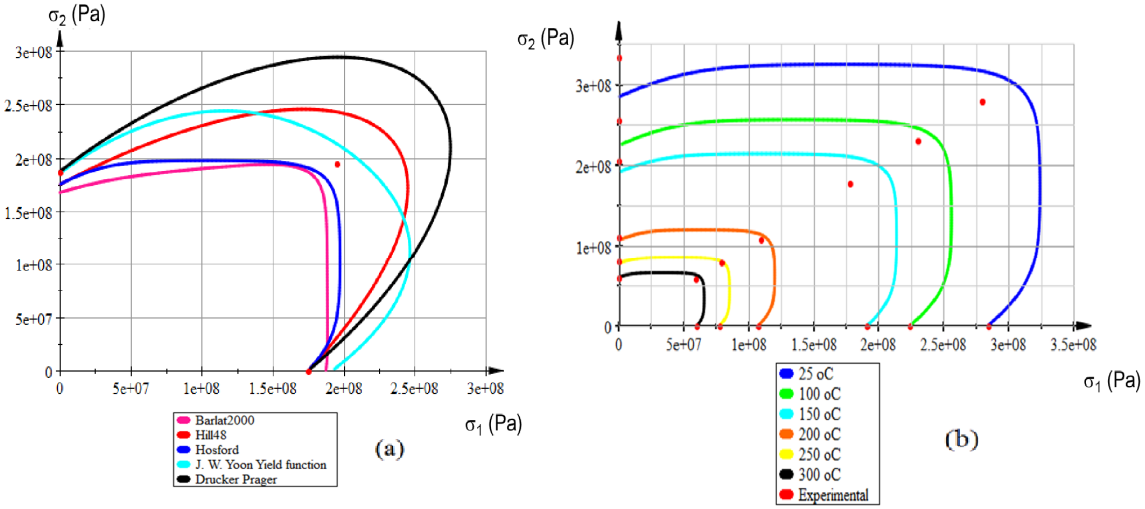

Figure 5. (a) Comparison of the different yield criteria of magnesium alloy AZ31B at RT, (b) Barlat2000 yield criterion of magnesium alloy AZ31B at various temperatures

Table 2. Barlat2000 anisotropy parameters at various temperatures

t°(°C)	α_1	α_2	α_3	α_4	α_5	α_6	α_7	α_8
25	0.6095	1.4078	0.8950	0.9785	1.0839	0.9912	1.7455	1.4159
100	0.5140	1.3024	0.7997	0.9884	0.9905	1.0024	1.6656	1.3667
150	0.5103	1.2894	0.8138	0.9889	0.9987	1.0041	1.6483	1.3727
200	0.5116	1.3067	0.8040	0.9965	1.0004	1.0078	1.6018	1.3972
250	0.4930	1.3172	0.8035	1.0148	1.0133	1.0129	1.5919	1.4155

2.2. Yield function

The Yld2000-2D yield function was proposed by Barlat et al in 2003 to consider anisotropy for sheet metals as below [7]:

$$\phi = \phi' + \phi'' = 2\sigma_s^a \quad (4)$$

$$\phi' = \left|X_1' - X_2'\right|^a,\ \phi'' = \left|2X_2'' + X_1''\right|^a + \left|2X_1'' + X_2''\right|^a \quad (5)$$

The exponent a is set to 6 for body center cubic (BCC) materials, 8 for face center cubic (FCC) and 10 for hexagon-closed packed (HCP), σ_s denote tensile yield stress, X_1', X_2' (or X_1'', X_2'') are the principal values of two deviatorics stress tensors $\mathbf{X}'$ and $\mathbf{X''}$ calculated by [7]:

$$\begin{aligned} \mathbf{X}' &= \mathbf{L}'\boldsymbol{\sigma} \\ \mathbf{X}'' &= \mathbf{L}''\boldsymbol{\sigma} \end{aligned} \quad \text{with } \boldsymbol{\sigma}^T = \left(\sigma_{xx}\ \sigma_{yy}\ \sigma_{xy}\right) \quad (6)$$

$$\mathbf{L}' = \begin{bmatrix} L_{11}' & L_{12}' & 0 \\ L_{21}' & L_{22}' & 0 \\ 0 & 0 & L_{66}' \end{bmatrix};\ \mathbf{L}'' = \begin{bmatrix} L_{11}'' & L_{12}'' & 0 \\ L_{21}'' & L_{22}'' & 0 \\ 0 & 0 & L_{66}'' \end{bmatrix}$$

$$\begin{bmatrix} L_{11}' \\ L_{12}' \\ L_{21}' \\ L_{22}' \\ L_{66}' \end{bmatrix} = \begin{bmatrix} 2/3 & 0 & 0 \\ -1/3 & 0 & 0 \\ 0 & -1/3 & 0 \\ 0 & 2/3 & 0 \\ 0 & 0 & 1 \end{bmatrix} \begin{bmatrix} \alpha_1 \\ \alpha_2 \\ \alpha_7 \end{bmatrix} \quad (7)$$

$$\begin{bmatrix} L_{11}'' \\ L_{12}'' \\ L_{21}'' \\ L_{22}'' \\ L_{66}'' \end{bmatrix} = \frac{1}{9} \begin{bmatrix} -2 & 2 & 8 & -2 & 0 \\ 1 & -4 & -4 & 4 & 0 \\ 4 & -4 & -4 & 1 & 0 \\ -2 & 8 & 2 & -2 & 0 \\ 0 & 0 & 0 & 0 & 9 \end{bmatrix} \begin{bmatrix} \alpha_3 \\ \alpha_4 \\ \alpha_5 \\ \alpha_6 \\ \alpha_8 \end{bmatrix}$$

Eight anisotropic parameters α_i (i = 1..8) are utilized to describe the anisotropy of sheet metals, modified in the yield Yld2000-2D function from experimental data should be calibrated from experimental data points such as tensile yield stress T_0, T_{45}, T_{90}, T_b = $(T_0+2*T_{45}+T_{90})/4$ and Lankford coefficients r_0, r_{45}, r_{90}, r_b = $(r_0+2*r_{45}+r_{90})/4$. 0°, 45°, 90° direction from RD.

These experimental data points are utilized to set up an error function as Eq.(8) [8], where V_i^{exp} and V_i^{pred} denote experimental values and predicted ones, respectively.

$$Err = \sum_1^8 \left(\frac{V_i^{exp}}{V_i^{Pred}} - 1 \right)^2 \quad (8)$$

The predicted uniaxial yield stress in θ-direction from RD is denoted as T_θ, are calculated as Eq.(9), and the predicted balanced biaxial tensile stress T_b is obtained as Eq.(10) [7]:

$$T_\theta = \frac{\sigma_s}{\left(\frac{\left|2K_{2p}'\right|^a + \left|3K_{1p}'' - K_{2p}''\right|^a + \left|3K_{1p}'' + K_{2p}''\right|}{2} \right)^{1/a}} \quad (9)$$

$$T_b = \frac{\sigma_s}{\left(\frac{\left(\frac{\alpha_1 - \alpha_2}{3}\right)^a + \left|L_{11}'' + 2L_{21}'' + L_{12}'' + 2L_{22}''\right|^a + \left|2L_{11}'' + L_{21}'' + 2L_{12}'' + L_{22}''\right|^a}{2} \right)^{1/a}} \quad (10)$$

The predicted r-value in θ-direction from RD under tension is denoted as r_θ which is calculated by Eq.(11), the predicted r_b-value in the balanced biaxial tension is defined the ratio of the strain increments in TD to that in RD in the balanced biaxial tension which is obtained as Eq.(12) [7]:

$$r_\theta = -\frac{\left(\partial\phi/\partial\sigma_{xx}\right)\sin^2\theta + \left(\partial\phi/\partial\sigma_{yy}\right)\cos^2\theta - \left(\partial\phi/\partial\sigma_{xy}\right)\sin\theta\cos\theta}{\left(\partial\phi/\partial\sigma_{xx}\right) + \left(\partial\phi/\partial\sigma_{yy}\right)} \quad (11)$$

$$r_b = \frac{d\varepsilon_{yy}}{d\varepsilon_{xx}} \text{ with } d\varepsilon_{yy} = d\lambda.\left(\frac{\partial\phi}{\partial\sigma_{xx}}\right) \text{ and } d\varepsilon_{xx} = d\lambda\left(\frac{\partial\phi}{\partial\sigma_{yy}}\right) \quad (12)$$

The error function of Eq.(8) is minimized by the Downhill Simplex method to identify the

Barlat2000 parameters [8]. This parameters are applied to rebuild the Barlat2000 yield locus in 2D coordinate (σ_1 , σ_2) at various temperatures, as shown Fig. 5(b) and Table 2. Yield locus also is shown in different yield criteria from classic to modern such as Hill48, Drucker Prager, Logan Hosford in Fig. 5(a).

3. FEA SIMULATION

3.1.Problem

Reference: The 8th International Conference and Workshop on Numerical Simulation of 3D Sheet Metal Forming Processes (21-26 August, 2011, Seoul, Korea): *"Benchmark 2 Simulation of the Cross-shaped Cup Deep-drawing Process"*; 51- 127.

3.2. Material model

The blank material is AZ31B magnesium alloy sheet with the thickness of 0.5 mm. Yield function, hardening curve, constitutive equation are defined from the material data by the approximate method in Section 2. Tensile test is at 25°C, 100°C, 150°C, 200°C, 250°C, 300°C, in each temperature with various strain rate: 0.16, 0.016, 0.0016 (s^{-1}). All the tool parts are made of

hardened tool steel SKD11.

3.3. Machine and tooling specifications

In order to maximize the deep-drawability of the blank material the die and the blank-holder are heated by heating cartridges embedded in each tool, while the punch and the pad are cooled by circulating water. Process parameters are as follows:

Surface temperature of the die and the blank-holder: 250℃, punch & pad: 100℃

Blank-holding force: 1.80 to 3.96 kN, pad force: 0.137 to 2.603 kN (linearly increases)

Drawing depth (punch displacement): over 18 mm, Punch velocity: 0.15 mm/s

Interface heat transfer coefficient: 4500 $W/m^2.C$, enthalpy: 107 KJ/Kg, conductivity: 96 W/m. C, specific heat: 1000 J/kg

3.4. FEA results:

Comparison of simulation results with experimental [8], as shown in Fig. 8. Thickness distribution of the formed part along at the punch displacements of 10 mm, as shown in Fig. 7(b)

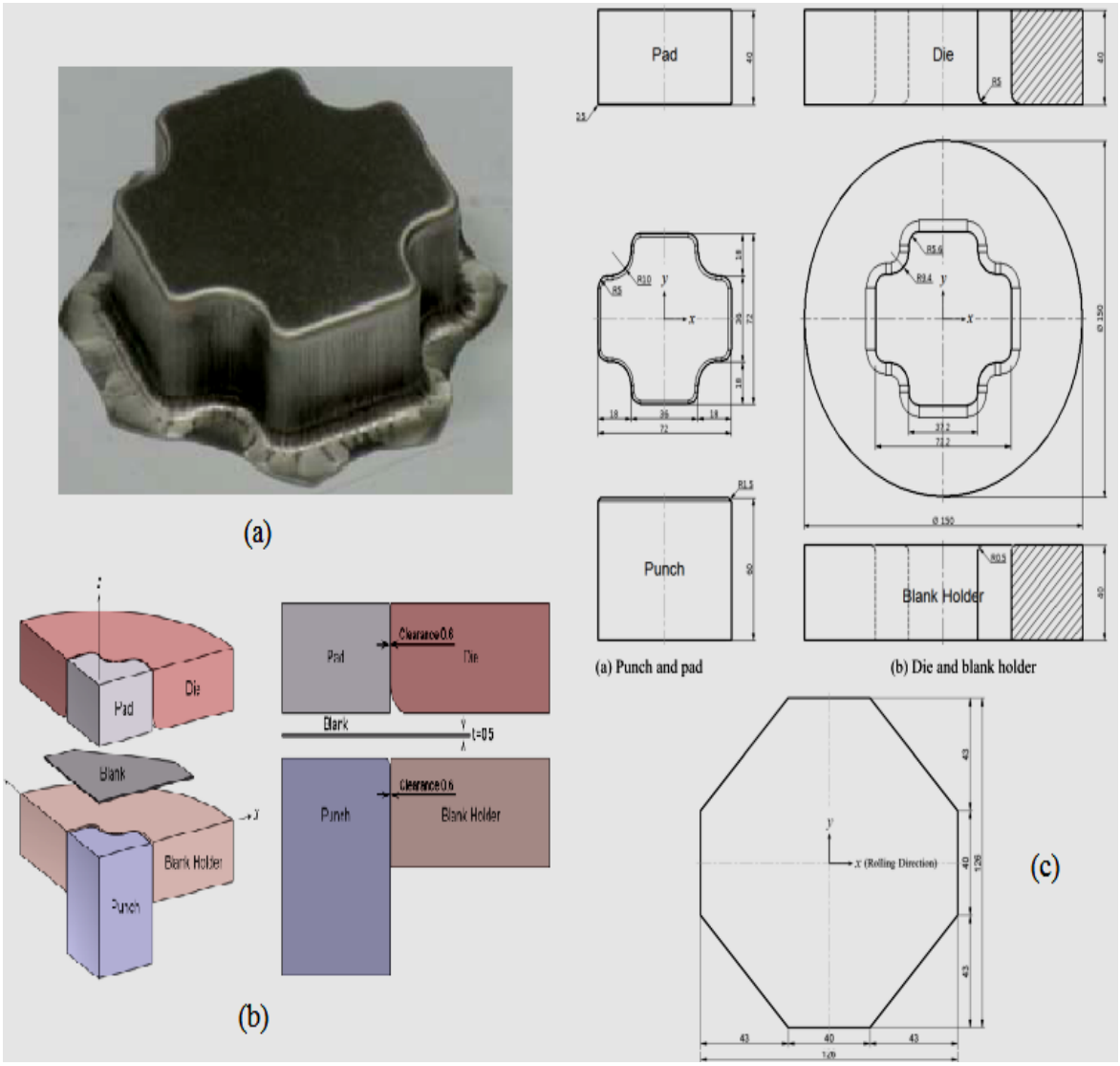

Fig. 6. (a) A cross-shaped deep-drawn cup, (b) Schematic view of the cross-shaped cup deep drawing process, (c) Geometry of the tools and the initial blank [9]

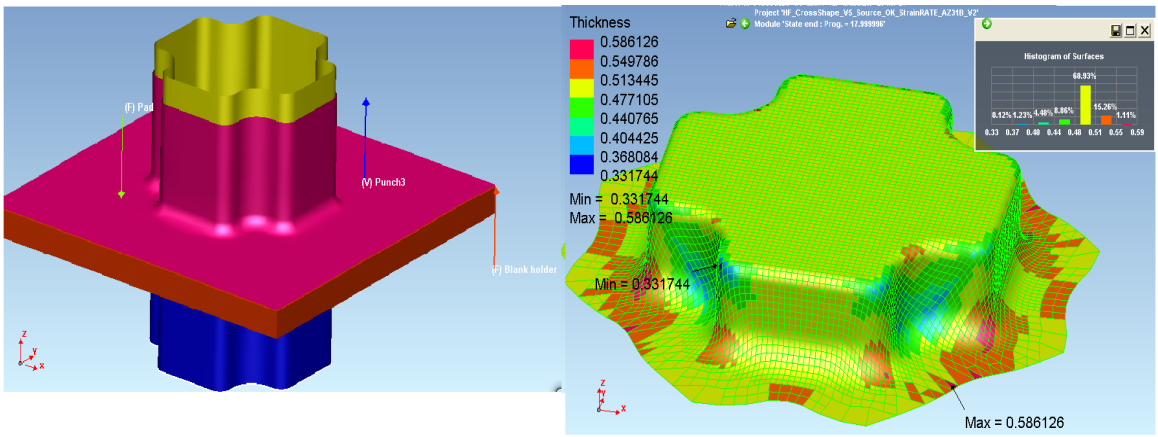

Figure. 7 (a) FEA modal in PAM- STAMP, (b) Thickness distribution of workpiece at the punch displacements of 18 mm

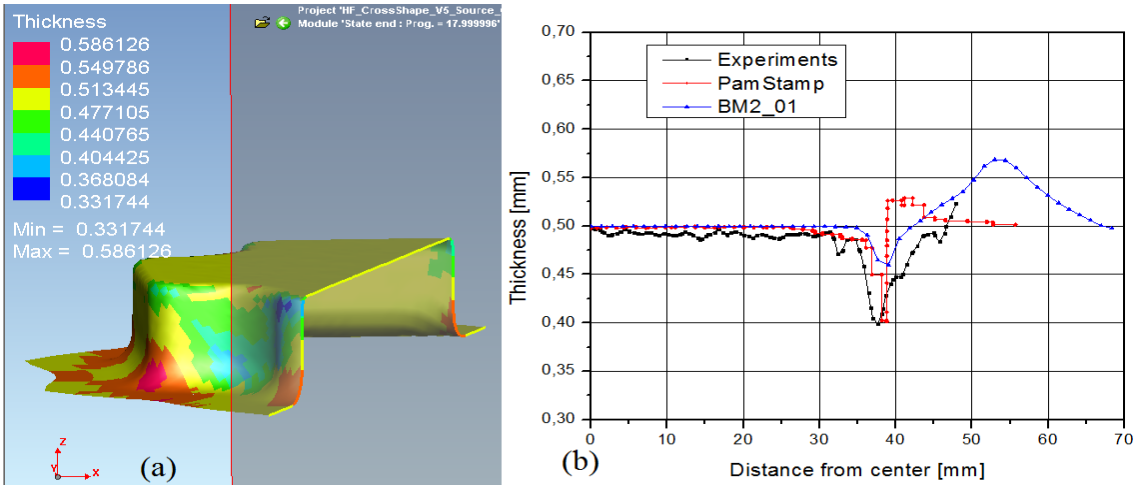

Figure. 8 (a) Thickness distrubution of workpiece on section by 67.5o of RD (b) Comparison of experiment and simulation thickness distrubution curves at the punch displacements of 18 mm (BM2_01- simulation result in LS- DYNA by other material model)

The Figure 8(a) shown section plane by 67.5º of rolling direction, thickness distrubution of this section were compared with the same section in experiment workpiece and simulation result using other material model (BM2_02 in LS- DYNA).

The predicted simulations shows that the lowest point of the curve is the thickness of blank- nose where is easiest to fracture Fig. 8 (b), some values greater than original thickness indicate the thickening on the flange.

4. CONCLUSIONS

The mechanical property of the magnesium AZ31B alloy sheet was characterized for its temperature-dependent hardening and different strain rate based on uniaxial tensile test data measured at 25ºC to 300ºC respectively. The proposed constitutive equations are described well the mechanical property of AZ31B sheet alloy when comparing the measurements and predictions. The approximated constitutive equations were implemented in FEA simulation The hot forming process FEA simulation of AZ31B sheet alloy using software PAM- STAMP 2G 2012. The following conclusions are obtained:

1. Flow stress equation of AZ31B using Ramgber-Osgood model is good fit to the measured results at the strain hardening stage in tensile test. The temperature- dependent constitutive equations and different strain rate could use to determine hardening behavior without the tensile testing. Using the exponential relationship to describe the hardening curve is good fit in work hardening before the peak stress, the peak stress decreases with decreasing strain rate, and the work hardening rate is significantly reduced before the peak stress, while the softening stage becomes longer after the peak stress, so, approximating in lower strain rate is considerable difference . The softening behavior which requires further study in the future.

2. Yield locus was also studied with different yield criteria. The results show that Barlat2000 yield criterion can well describe anisotropy yield locus in tensile test for AZ31B sheet at various temperatures. Yld2000-2D should be very well received by FE implementers and users for numerical simulations of sheet forming processes because of its accuracy and simplicity.

3. The predicted simulations is conformed well with experiment results. This proves good description of constitutive equations.

Xác định mô hình vật liệu ở nhiệt độ cao với tốc độ biến dạng khác nhau và mô phỏng quá trình gia công nóng cho tấm hợp kim Mg AZ31B

- **Trương Tích Thiện**
- **Nguyễn Thành Long**
- **Vũ Nguyễn Thanh Bình**
- **Nguyễn Thái Hiền**

Trường Đại học Bách Khoa, ĐHQG-HCM

TÓM TẮT:

Gần đây hợp Magie là một trong những hợp kim nhẹ được nghiên cứu rộng rãi vì tính dẻo và khả năng tạo hình ở nhiệt độ cao, việc giảm khối lượng các chi tiết trong khi vẫn giữ được yêu cầu về mặt chức năng là một trong những mục tiêu chính trong các ngành công nghiệp nhằm tiết kiệm nguyên vật liệu, năng lượng và chi phí, … Đối tượng nghiên cứu là tấm hợp kim AZ31B (3% Al và 1% Zn), tỷ trọng khoảng 2/3 of hợp kim nhôm và khoảng 1/4 of thép. Tuy nhiên, vì cấu trúc tinh thể lục phương xếp chặt HCP (Hexagonal Close-Packed), hợp kim Mg có tính dẻo kém ở nhiệt độ phòng. Từ số liệu thí nghiệm kéo đơn trục hợp kim AZ31B với các tốc độ biến dạng khác nhau tại nhiều nhiệt độ, các phương trình đường cong ứng suất biến dạng được xác đinh theo mô hình Ramgberg- Osgood để phù hợp với kế quả thí nghiệm. Quỹ đạo chảy cũng được xác định trên mặt phẳng chảy $\sigma 1$-$\sigma 2$ với những tiêu chuẩn chảy khác nhau Hill48, Drucker Prager, Logan Hosford, Y. W. Yoon 2013 và riêng tiêu chẩn chảy Barlat 2000 ở nhiều nhiều nhiệt độ khác nhau. Áp dụng những phương trình cơ bản đã xác định tại nhiều nhiệt độ và tốc độ biến dạng khác nhau, việc mô phỏng phần tử hữu hạn quá trình dập tấm hợp kim AZ31B trên phần mềm PAM-STAMP 2G 2012, để kiểm chứng mô hình vật liệu và các phương trình cơ bản.

Từ khóa: *Tấm hợp kim Mg, AZ31B, phương trình cơ bản, biến cứng, Ramgberg- Osgood, Barlat 2000, phương pháp PTHH.*

REFERENCES

[1]. S. H. Zang, K. Zang, C. A. Lee, M. G. Lee, J. H. Kim, H. Y. Kim. *Mechanical Behavior of AZ31B Mg Alloy Sheets under Monotonic and Cyclic Loadings at Room and Moderately Elevated Temperatures*, Journal of Materials (2014); 1271- 1295.

[2]. J. H. Kim, D. Kim, Y. S. Lee, M. G. Lee, K. Chung, H. Y. Kim, R. H. Wagoner. *A temperature- dependent elasto- plastic constitutive model for magnesium alloy AZ31 sheets*. International Journal of Plasticity(2013); 66-93.

[3]. R. Neugebauer, T. Altan, M. Geiger, M. Geiger, M. Kleiner, A. Sterzing. *Sheet metal forming at elevated temperatures*. CIRP

Annals – Manufacturing Technology (2006), Volume 55, Issue 2; 793-816.

[4]. X.Y. Lou, M. Li, R. K. Boger, S. R. Agnew, R.H Wagoner. *Hardening evolution of AZ31B Mg sheet.* International Journal of Plasticity(2007); 44-86

[5]. W. Ramberg, W. R. Osgood. *Description of stress- strain curves by three parameters*. Technical notes National advisory committee for aeronautics (1943).

[6]. N. T. Nguyen, O. S. Seo, C. A. Lee, M. G. Lee, J. H. Kim, H. Y. Kim. *Mechanical Behavior of AZ31B Mg Alloy Sheets under Monotonic and Cyclic Loadings at Room and Moderately Elevated Temperatures*. Journal of Materials(2014); 1271- 1295.

[7]. F. Barlat, J. C. Brem. *Plane stress yield function for aluminum alloy sheets-part 1: theory*. International Journal of Plasticity(2003), Vol.19; 1297-1319.

[8]. J. W. Yoon, Y. Lou, J. Yoon, M. V. Glazoff. *Asymmetric yield function based on the stress invariants for pressure sensitive metals.* International Journal of Plasticity(2013)

[9]. H. Huh, K. Chung, S. S. Han, W. J. Chung. *Benchmark 2 Simulation of the Cross-shaped Cup Deep-drawing Process.* The 8th International Conference and Workshop on Numerical Simulation of 3D Sheet Metal Forming Processes (21-26 August, 2011, Seoul, Korea); 51- 127